Research Article | Vol. 25, No. 9 | 1 May 2017 | OPTICS EXPRESS 9535

Optics EXPRESS

Reflection sensitivity of 1.3 μm quantum dot lasers epitaxially grown on silicon

ALAN Y. LIU,[1,*] TIN KOMLJENOVIC,[2] MICHAEL L. DAVENPORT,[2] ARTHUR C. GOSSARD,[1,2] AND JOHN E. BOWERS[1,2]

[1]*Materials Department, University of California Santa Barbara, Santa Barbara, California, 93106, USA*
[2]*Department of Electrical and Computer Engineering, University of California Santa Barbara, Santa Barbara, California, 93106, USA*
[*]*ayliu01@engineering.ucsb.edu*

Abstract: We present measurements of relative intensity noise versus various levels of optical feedback for 1.3 μm quantum dot lasers epitaxially grown on silicon for the first time. A systematic comparison is made with heterogeneously integrated 1.55 μm quantum well lasers on silicon. Our results indicate up to 20 dB reduced sensitivity of the quantum dot lasers on silicon compared to the quantum wells.

OCIS codes: (140.5960) Semiconductor lasers; (250.0250) Optoelectronics.

References and links

1. Z. Zhou, B. Yin, and J. Michel, "On-chip light sources for silicon photonics," Light Sci. Appl. **4**, e358 (2015).
2. M. J. Heck and J. E. Bowers, "Energy efficient and energy proportional optical interconnects for multi-core processors: Driving the need for on-chip sources," IEEE J. Sel. Top. Quantum Electron. **20**, 332–343 (2014).
3. R. Tkach and A. Chraplyvy, "Regimes of feedback effects in 1.5-μm distributed feedback lasers," J. Lightwave Technol. **4**, 1655–1661 (1986).
4. T. Komljenovic, S. Srinivasan, E. Norberg, M. Davenport, G. Fish, and J. E. Bowers, "Widely tunable narrow-linewidth monolithically integrated external-cavity semiconductor lasers," IEEE J. Sel. Top. Quantum Electron. **21**, 214–222 (2015).
5. D. Huang, P. Pintus, C. Zhang, Y. Shoji, T. Mizumoto, and J. E. Bowers, "Electrically driven and thermally tunable integrated optical isolators for silicon photonics," IEEE J. Sel. Top. Quantum Electron. **22**, 1–8 (2016).
6. D. O'Brien, S. P. Hegarty, G. Huyet, J. G. McInerney, T. Kettler, M. Laemmlin, D. Bimberg, V. M. Ustinov, A. E. Zhukov, S. S. Mikhrin, and A. R. Kovsh, "Feedback sensitivity of 1.3 μm InAs/GaAs quantum dot lasers," Electron. Lett. **39**, 1819–1820 (2003).
7. G. Huyet, D. O'Brien, S. P. Hegarty, J. G. McInerney, A. V. Uskov, D. Bimberg, C. Ribbat, V. M. Ustinov, A. E. Zhukov, S. S. Mikhrin, A. R. Kovsh, J. K. White, K. Hinzer, and A. J. SpringThorpe, "Quantum dot semiconductor lasers with optical feedback," Phys. Stat. Sol. **201**, 345–352 (2004).
8. D. O'Brien, S. P. Hegarty, G. Huyet, A. V. Uskov, "Sensitivity of quantum-dot semiconductor lasers to optical feedback", Opt. Lett. , **29**, 1072–1074 (2004).
9. S. Melnik, G. Huyet, and A. V. Uskov, "The linewidth enhancement factor α of quantum dot semiconductor lasers," Opt. Express **14**, 2950–2955 (2006).
10. C. Otto, *Dynamics of Quantum Dot Lasers: Effects of Optical Feedback and External Optical Injection* (Springer Science and Business Media, 2014).
11. J. Helms and K. Petermann, "A simple analytic expression for the stable operation range of laser diodes with optical feedback," IEEE J. Quantum Electron. **26**, 833–836 (1990).
12. A. Zhukov, M. Maksimov, and A. Kovsh, "Device characteristics of long-wavelength lasers based on self-organized quantum dots," Semiconductors **46**, 1225–1250 (2012).
13. L. A. Coldren, S. W. Corzine, and M. L. Mashanovitch, *Diode Lasers and Photonic Integrated Circuits*, vol. 218 (John Wiley and Sons, 2012).
14. J. Wang and K. Petermann, "Noise analysis of semiconductor lasers within the coherence collapse regime," IEEE J. Quantum Electron. **27**, 3–9 (1991).
15. A. Y. Liu, C. Zhang, J. Norman, A. Snyder, D. Lubyshev, J. M. Fastenau, A. W. Liu, A. C. Gossard, and J. E. Bowers, "High performance continuous wave 1.3 μm quantum dot lasers on silicon," Appl. Phys. Lett. **104**, 041104 (2014).
16. A. Y. Liu, S. Srinivasan, J. Norman, A. C. Gossard, and J. E. Bowers, "Quantum dot lasers for silicon photonics [Invited]," Photon. Res. **3**, B1–B9 (2015).
17. S. Chen, W. Li, J. Wu, Q. Jiang, M. Tang, S. Shutts, S. N. Elliott, A. Sobiesierski, A. J. Seeds, I. Ross, P. M. Smowton, and H. Liu, "Electrically pumped continuous-wave III-V quantum dot lasers on silicon," Nat. Photonics **10**, 307–311 (2016).

#282381 https://doi.org/10.1364/OE.25.009535
Journal © 2017 Received 8 Dec 2016; revised 9 Feb 2017; accepted 1 Mar 2017; published 18 Apr 2017

Optics EXPRESS

18. A. Y. Liu, J. Peters, X. Huang, D. Jung, J. Norman, M. L. Lee, A. C. Gossard, and J. E. Bowers, "Electrically pumped continuous-wave 1.3 μm quantum-dot lasers epitaxially grown on on-axis (001) GaP/Si," Opt. Lett. **42**, 338–341, (2017).
19. O. Ueda and S. Pearton, *Materials and Reliability Handbook for Semiconductor Optical and Electron Devices* (Springer, 2014).
20. M. L. Davenport, S. Skendzic, N. Volet, J. C. Hulme, M. J. Heck, and J. E. Bowers, "Heterogeneous silicon/III-V semiconductor optical amplifiers," IEEE J. Sel. Top. Quantum Electron. **22**, 1–11 (2016).
21. D. Silvano, R. H. Horng, "The diagram of feedback regimes revisited," IEEE J. Sel. Top. Quantum Electron. **19**, 1500309 (2013).
22. T. Komljenovic, M. Tran, M. Belt, S. Gundavarapu, D. J. Blumenthal, and J. Bowers, "Frequency modulated lasers for interferometric optical gyroscopes," Opt. Lett. **41**, 1773–1776 (2016).
23. D. Y. Cong, A. Martinez, K. Merghem, G. Moreau, A. Lemaitre, J. G. Provost, O. L. Gouezigou, M. Fischer, I. Krestnikov, A. R. Kovsh, and A. Ramdane, "Optimisation of a-factor for quantum dot InAs/GaAs Fabry-Perot lasers emitting at 1.3 μm," Electron. Lett. **43**, 222–224 (2007).
24. K. Petermann, "External optical feedback phenomena in semiconductor lasers," IEEE J. Sel. Top. Quantum Electron. **1**, 480–489, (1995).

1. Introduction

On-chip lasers on silicon are necessary to meet techno-economic requirements of low cost, high device/bandwidth density, and low power consumption for high volume applications such as data communication [1, 2]. As an integrated component of a photonic integrated circuit and/or optical system, unintentional reflections from various possible interfaces such as active/passive transitions, waveguide crossings, regrowth interfaces, process imperfections, etc. can produce unwanted feedback to the laser. The behavior of quantum well lasers under optical feedback has been studied extensively, with a well known diagram classifying laser response under five distinct regimes of different feedback strengths and phases [3]. Outside of very narrow regimes where feedback is beneficial for inducing linewidth narrowing, the majority of feedback levels causes deleterious effects such as linewidth broadening, mode hopping, and/or increased amplitude noise [3, 4]. For data communication systems this would be undesirable as the increase in laser amplitude or phase noise would degrade the bit error rate. Lasers integrated with a silicon photonic chip are particularly susceptible to these effects, as the low loss waveguides and high index contrast inherent to the platform are particularly conducive to the creation of strong unintentional feedback. External isolators have traditionally been used to limit unwanted feedback to the laser, and silicon based on-chip isolators have been recently demonstrated with maximum isolation ratios up to 32 dB [5]. However, the integration of an isolator increases cost, process complexity, total chip/system size, and total loss within the system. The ability to operate the laser without an isolator is desirable from both an economic as well as system performance point of view.

1.1. Feedback sensitivity of InAs quantum dot lasers on GaAs

Previous studies have indicated that 1.3 μm InAs/GaAs quantum dot lasers on native GaAs substrates can be more tolerant to feedback than is expected from quantum wells. For example, a fairly high coherence collapse threshold of -8 dB was previously reported in [6] for an 1.3 μm InAs quantum dot laser on GaAs, which is 20-30 dB higher than what is measured for an AlGaInAs quantum well laser [7]. Theoretical treatments on the dynamics within InAs/GaAs quantum dot lasers have correlated this behavior to the highly damped relaxation oscillations and lower amplitude-phase coupling (α) factors in quantum dot lasers relative to quantum wells [7–10]. This is illustrated in Fig. 1 which plots numerical evaluations of the common analytical expression for predicting the critical feedback level where the laser enters a coherence collapse regime as derived in [11]:

$$f_{crit} = \frac{\tau_L^2 (K f_r^2 + \gamma_0)^2}{16|C_e|^2} \left(\frac{1+\alpha^2}{\alpha^4} \right) \tag{1}$$

Optics EXPRESS

where τ_L is the roundtrip delay within the gain cavity, α the linewidth enhancement factor, $|C_e| = \frac{1-R}{2\sqrt{R}}$ the coupling strength from the laser cavity to the external cavity, $\gamma = (Kf_r^2 + \gamma_0)$ is the damping rate of the relaxation oscillations with f_r being the resonance frequency, K the K-factor, and γ_0 is the damping factor offset. Feedback is defined as the ratio of the reflected power over the emitted power. Fig. 1 plots Eq. 1 for two different values of the K factor characteristic of either quantum dot lasers (K=1 ns) [12] or quantum well lasers (K=0.265 ns) [13], with everything else kept the same. As can be seen, the difference in the K factor alone is predicted to result in a 10 dB increase in f_{crit} for quantum dot lasers relative to quantum wells, with any differences due to the α factor between dots and wells resulting in even larger increases to the critical feedback level for coherence collapse. Furthermore, the peak relative intensity noise (RIN) of semiconductor lasers under optical feedback is capped by the inverse of the damping rate of relaxation oscillations: $\text{RIN}_{peak} = \frac{1}{\gamma}$ [14]. Thus, feedback induced noise is expected to be highly suppressed in quantum dots lasers as well.

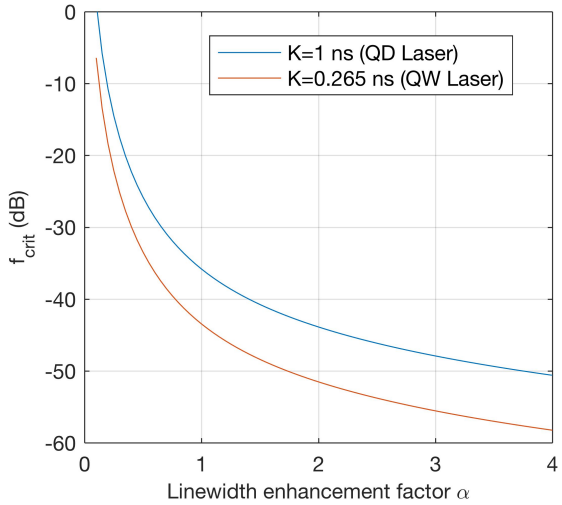

Fig. 1. A numerical evaluation of Eq. 1 for two different values of the K factor characteristic of either quantum dot lasers (K=1 ns) [12] or quantum well lasers (K=0.265 ns) [13], with everything else kept the same (τ_L=4 ps, f_r=3 GHz, γ_0=0.65 GHz, R=0.3.

1.2. *Motivation for this study*

Recent reports on the static performance of III-V quantum dot lasers epitaxially grown on silicon show that they are a promising monolithic light source for silicon photonics, with the potential to be manufactured at large scale with low cost [15–18]. As outlined earlier in the introduction, there is significant value in being able to operate these lasers without an isolator for future integrated communication systems. Although the feedback sensitivity of quantum dot lasers on GaAs has been studied and is understood, one cannot *a priori* that the dynamic properties for quantum dot lasers grown on silicon will be the same as their native substrate counterparts. The aforementioned properties of feedback tolerance inherent to quantum dots on native substrates arises due to the unique carrier dynamics present in quantum dot active regions. For quantum dot lasers epitaxially grown on silicon, however, the dislocation density present in the active region is typically 4-5 orders of magnitude larger than on native GaAs substrates ($> 10^8$ cm^{-2} on Si vs $< 10^4$ cm^{-2} on GaAs). The energy states associated with dislocations are known to be able to scatter or trap carriers, as well as absorb photons in the lasing cavity [19]. It is unknown how

these perturbations to the carrier and photon populations will affect the relative intensity noise and feedback dynamics within the laser. In this work, we will seek to experimentally quantify for the first time the reflection sensitivity of quantum dot lasers epitaxially grown on silicon by measuring their relative intensity noise under different levels of feedback. As our study is framed in the context of silicon photonics, we will also present a systematic comparison with quantum well lasers heterogeneously integrated on silicon measured with the same setup, which has not been done before.

2. Experimental methods

2.1. Experimental setup

The measurement setup used is shown in Fig. 2. Light from the device under test (DUT) is first coupled to a lensed fiber and split by a 50:50 directional fiber coupler. The power in one arm is fed into a spectrum analyzer to monitor the relative intensity noise, and an optical isolator with 60 dB of isolation ratio isolates the DUT from uncontrolled reflections. Power in the other arm is reflected back to the DUT with a Faraday mirror, which along with an in-line Faraday rotator provides a total round-trip polarization shift of 180 degrees (45 degree single pass rotation from each component). This ensures that any changes to the original polarization state of the output light caused by fiber birefringence will be undone on the return trip, ensuring that the polarization of the feedback is nearly the same as the original output. The amplitude of the feedback is controlled with an in-line variable optical attenuator. A 1% fiber coupler tap right after the lensed fiber monitors the power levels in the forward and backward directions, and the feedback level is defined as the ratio of the backward to forward powers measured by the monitor photodiodes connected to the taps. The fiber couplers were dual-band couplers for operation near 1550 and 1310 nm, while the other wavelength sensitive components (isolator, Faraday rotator, and Faraday Mirror) were swapped out as needed for the wavelength of the DUT. With the exception of the spectrum analyzer interface, all the fiber connections had angled connectors. The external cavity round trip path length is roughly 13 meters for the quantum well devices, and 15 meters for the quantum dot lasers, due to different fiber pigtail lengths of the components used. For this study, we examined the relative intensity noise (RIN) spectrum from 100 MHz to 10 GHz. This range of frequencies was chosen to be within the highest sensitivity range of the spectrum analyzer. Resolution bandwidth was 3 MHz for all measurements.

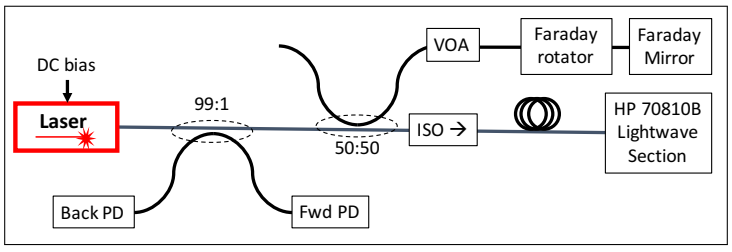

Fig. 2. A schematic of the measurement setup used in this study.

2.2. Devices studied

1.3 μm InAs/GaAs based quantum dot lasers epitaxially grown on GaP/Si substrates and 1.5 μm AlGaInAs quantum well lasers heterogeneously integrated on silicon are compared. The make-up and fabrication of the quantum dot and quantum well lasers on silicon in this study have been previously reported [18, 20]. To make the comparison as fair as possible, the quantum dot and quantum well devices used in this study were down-selected from available devices

Optics EXPRESS

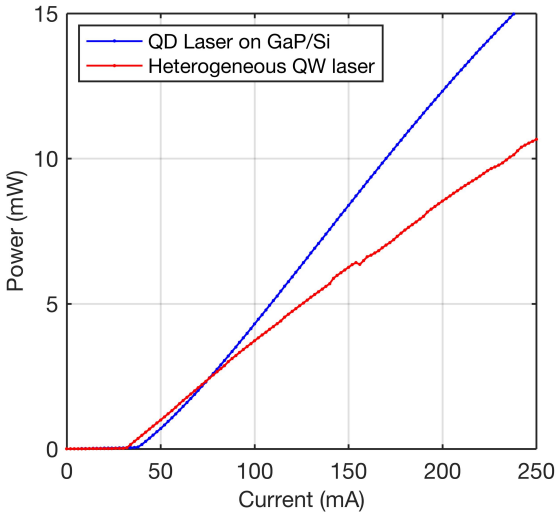

Fig. 3. Typical light-current characteristics of the quantum dot lasers on GaP/Si and heterogeneously integrated quantum well lasers in this study.

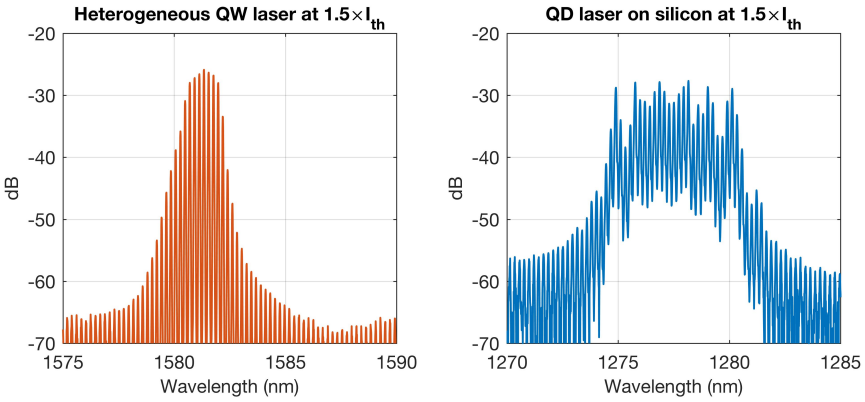

Fig. 4. Lasing spectra at 20°C from a heterogeneously integrated quantum well laser on silicon (left - biased at 48 mA) and a quantum dot laser on silicon (right - biased at 57 mA) used in this study. Multiple longitudinal Fabry-Perot modes are visible in each case.

Optics EXPRESS

in our lab with the criteria that they both be of similar type (in this case Fabry-Perot), have similar cavity lengths (due to the implicit dependence of f_{crit} on the length of the gain section through τ_L), and operating in or close to single transverse mode. The heterogeneously integrated quantum well lasers studied have 7 compressively strained InAlGaAs quantum wells as the active region, lasing around 1580 nm at room temperature (RT). These lasers are roughly 1560 μm in length with 1048μm long III-V gain sections (as measured from taper to taper) and the rest being purely passive silicon waveguide sections [20]. The III-V mesa widths are 26 μm wide with implant defined current channel width of 4 μm. The quantum dot lasers measured are deeply etched ridge waveguide lasers epitaxially grown on GaP/silicon substrates around 1 mm long in length and 3-3.5 μm in width, with 7 layers of InAs/GaAs quantum dots as the active region, and lasing around 1280 nm at RT. The output facet for the quantum well lasers is an uncoated silicon waveguide facet with $\sim$ 30% reflectivity, whereas for the quantum dot lasers it is a coated III-V facet with approximately $\sim$ 55% reflectivity. Figure 3 shows typical measured light-versus-current plots for the two types of lasers, and representative lasing spectra for the two types of lasers are shown in Fig. 4. Because the external cavity delay time is much longer than the time scale of the relaxation oscillations ($L_{ext} > c/(2f_r)$) - where in this case $L_{ext} \geq$ 13 m and $c/(2f_r) \sim$ 7.5 cm assuming f_r to be 2 GHz - we expect the feedback behavior to be independent of the feedback phase [21]. The coherence length of multi-mode Fabry-Perot lasers are typically on the order of a few to tens of cms [22], which is more than two orders of magnitude shorter than the external cavity length of our setup. The feedback can therefore be assumed to be incoherent with the emitted radiation as well.

3. Results and discussion

Because both α and f_r have a dependance on the applied current density, we study the effect of feedback on the RIN at several different bias points above threshold. In particular, the α factor of quantum dot lasers tend to have a strong dependance on current due to saturation effects [9, 23]. We found during our studies that the low frequency noise is the most sensitive to optical feedback. Figure 5 shows the low frequency laser RIN at 100 MHz (with thermal and shot noise subtracted out) for two different heterogeneously integrated quantum well lasers compared to two different quantum dot lasers on silicon, each subjected feedback levels varying approximately from -60 to -10 dB. For each laser, RIN was measured for five different bias currents (and corresponding output powers). Of note is the observation that the low frequency RIN at 100 MHz for the quantum well lasers show a sharp increase with increasing feedback for each bias current, up to 30 dB. On the other hand, RIN for the quantum dot lasers show a saturation behavior with increasing feedback, with the largest increase for each bias current being roughly 10 dB within the same measurement range. The RIN values of the quantum dot lasers at the highest level of feedback (-10 dB) are matched by the quantum well lasers at nearly 20 dB weaker feedback levels (-30 dB). The coherence collapse threshold can be estimated by the point at which the RIN starts to sharply increase versus increasing feedback [24]. We estimate that the threshold is between -40 to -30 dB for the heterogeneously integrated quantum well lasers studied here, which agrees well with previous reports of traditional III-V quantum well lasers [24]. However it is more difficult to estimate for the quantum dot lasers as the RIN increase is much smaller. A more precise determination may be made by examining a high resolution optical spectra for the appearance of satellite modes appearing at roughly multiples of the relaxation oscillation frequency away from the main lasing mode [3]. However we are limited in the pursuit of this endeavor by our current setup and the resolution available on our optical spectrum analyzer.

Figure 6 shows the measured system RIN - the sum of laser, thermal, and shot noise - of a heterogeneously integrated quantum well laser as well as a quantum dot laser, both biased at $1.5\times I_{th}$. In each case, RIN was measured at the maximum and minimum attainable values of feedback with our testing setup. In the weak feedback limit ($\sim$-60 dB), the laser RIN of both

Optics EXPRESS

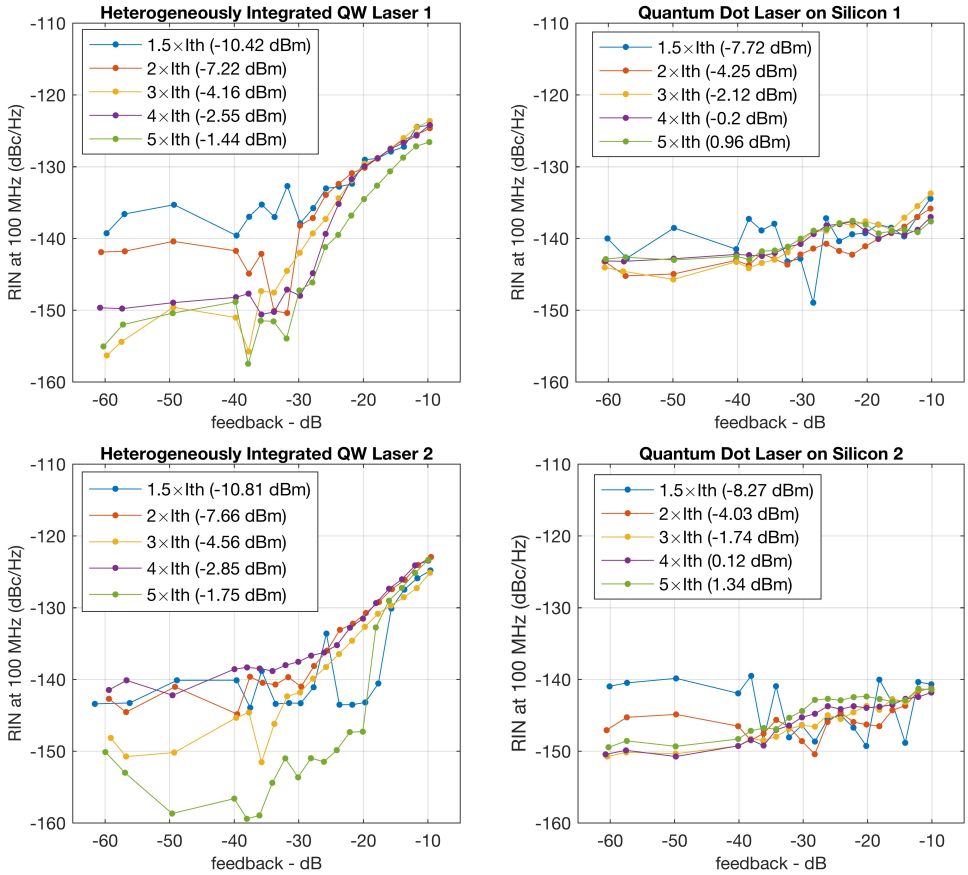

Fig. 5. Laser RIN at 100 MHz with thermal and shot noise subtracted out versus various levels of optical feedback for two different heterogeneously integrated quantum well lasers (left) and two different quantum dot lasers on silicon (right). The legend indicates the bias current applied to the laser as well as the optical power received at the spectrometer. While the quantum well lasers sometimes exhibit increases in RIN up to 30 dB over the range of feedback values, the variation in RIN for the quantum dot lasers is limited to within 10 dB the measured bias currents.

lasers is below the thermal noise floor and the spectrum - essentially the thermal noise - is fairly flat. In the strong feedback limit (~ -10 dB), the RIN spectrum for the quantum well laser exhibits groups of large spikes in the RIN spectrum separated by presumably the relaxation oscillation frequency of roughly 2 GHz, the value of which is close to what has been previously measured for other heterogeneously integrated quantum well lasers [4]. The RIN spectrum for the quantum dot lasers is almost unchanged, with only a small increase in the low frequency RIN. Figure 7 shows the low frequency RIN for both lasers at $2\times I_{th}$ from 100 to 200 MHz, averaged over 10 scans to better resolve the spectral features. Under strong feedback, enhanced RIN peaks separated by ostensibly the external cavity roundtrip frequency are visible for both types of lasers, with a slightly smaller spacing for the quantum dot laser due to the longer external cavity length. In agreement with the data shown in Fig. 5, the overall increase in RIN is lower for the quantum dot laser over the frequency range measured. Along with the data presented in Fig. 6, we can conclude that the increase in total integrated RIN induced by optical feedback is much lower for quantum dot lasers relative to the quantum well lasers.

Optics EXPRESS

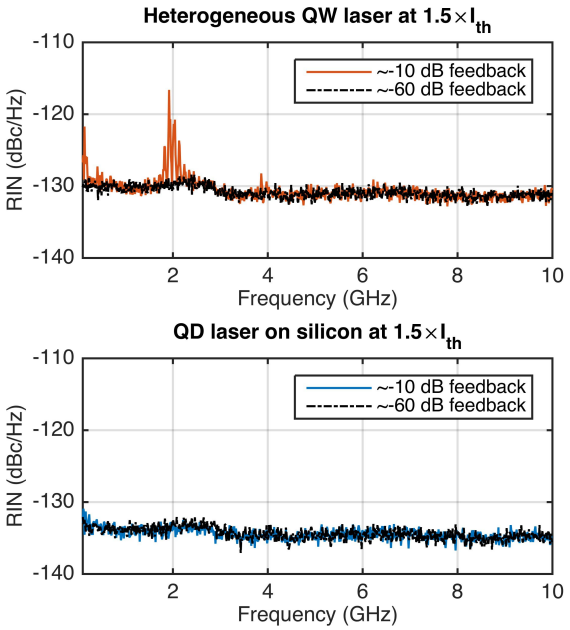

Fig. 6. Total system RIN from 100 MHz to 10 GHz, for quantum well and quantum dot lasers biased at $1.5\times I_{th}$. The feedback induces strongly enhanced RIN peaks in the noise spectra of the quantum well laser, with the peak around 2 GHz presumably related to the relaxation oscillation frequency. Similar features are not visible in the case of the quantum dot lasers.

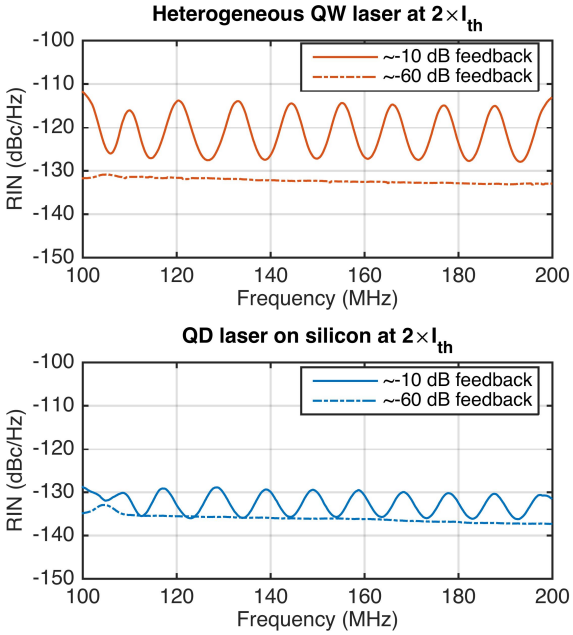

Fig. 7. Measured low frequency system RIN at weak and strong feedback levels at $2\times I_{th}$. Enhanced RIN peaks are visible under strong feedback for both types of lasers at frequencies separated by the external cavity roundtrip frequency. However the increase under strong feedback is much less for the quantum dot laser.

Optics EXPRESS

4. Conclusion

In summary, we have studied the reflection sensitivity of quantum dot lasers epitaxially grown on silicon for the first time. Compared to heterogeneously integrated quantum wells, the quantum dot lasers show nearly 20 dB reduced sensitivity to feedback while maintaining low levels of RIN over the entire feedback range. These results are consistent with previous studies of 1.3 μm quantum dot lasers on native GaAs substrates, indicating that the dynamic properties of quantum dot lasers directly grown on silicon may be largely unperturbed relative to their native substrate counterparts. These results demonstrate the potential for isolator free operation of quantum dot lasers directly grown on silicon for future silicon photonics systems.

Funding

Advanced Research Projects Agency-Energy (ARPA-E) (DE-Ar0000672).

Acknowledgments

We thank Dr. Mike Haney for his support of this program.